MOLECULAR PHYSICS, 2002, VOL. 100, NO. 22, 3513–3519

Three-photon absorption spectroscopy: the L($^1\Phi_3$) and m($^3\Pi_1$) states of HCl and DCl

ÁGÚST KVARAN* and HUASHENG WANG
Science Institute, University of Iceland, Dunhaga 3, 107 Reykjavík, Iceland

(*Received 3 January 2002; revised version accepted 16 April 2002*)

Analysis of (3+1) REMPI room temperature spectra by use of three-photon absorption modelling allowed, for the first time, identification and characterization of $\Omega = 3$, Φ states (L($^1\Phi_3$)) in HCl and DCl and of the m($^3\Pi_1$) state in DCl. Simulation analyses and determination of isotope shifts allowed evaluation of vibrational and rotational spectroscopic parameters for both states and both molecules. The mechanism of three-photon absorption in the m($^3\Pi_1$) X($^1\Sigma^+$) transition is discussed.

1. Introduction

(3+1) REMPI (resonance-enhanced multiphoton ionization) involves three-photon resonance absorption followed by one-photon ionization. Recently (3+1) REMPI spectra of rotational structure in electronic transitions of diatomic molecules have been simulated successfully by taking account of the three-photon transition probabilities only [1–3]. This suggests that the final ionization step is largely wavelength independent and that the (3+1) REMPI spectra can be treated as three-photon absorption spectra to a first approximation. Furthermore, three-photon absorption spectroscopy analysis of (3+1) REMPI spectra has recently proven successful at detecting states 'hidden' in the more commonly used single-, and two-photon absorption techniques [1–3]. Thus the lowest energy $\Omega = 3$, Φ states of HBr ($l^3\Phi_3\{4d\delta\}$; $\tilde{\nu}^0 = 80\,167\,cm^{-1}$ for $v' = 0$ and $L^1\Phi_3\{4d\delta\}$; $\tilde{\nu}^0 = 82\,837\,cm^{-1}$ for $v' = 0$) were detected and analysed in (3+1) REMPI spectra recorded at room temperature [1, 2] and a number of higher energy $\Omega = 3$ (Φ) states were observed in cold supersonic expansions [3]. Three-photon absorption spectroscopy has added to the rich spectroscopy of the hydrogen halides which is characterized by a wide variation in the strengths of Rydberg to ion-pair interactions as well as spin–orbit couplings arising from the halogen atoms [4–9]. Furthermore, use of expressions for rovibrational line strengths in three-photon absorption [1, 2] has been found to be useful to derive rotational population distributions in the ground states of HBr [2] and HCl [10] from (3+1) REMPI spectra. The relative intensities of rotational line series have been used as evidence in debates about the effect of intermediate states on the mechanism of multiphoton processes in two- [7, 8, 11] and three- [2] photon absorptions to $\Omega' = 0$ $\Omega'' = 0$ transitions in Br_2 [11], HBr [7] and HCl [2, 7, 8].

In this paper we present for the first time observation and analyses of electronic states in HCl and DCl which are not accessible in one- and two-photon spectra. Hönl–London expressions are used to identify and analyse $\Omega = 3$, Φ states of HCl and DCl from their (3+1) REMPI room temperature spectra. The states are assigned as the $L^1\Phi_3$ Rydberg states corresponding to the principal quantum number 3, belonging to the dδ manifold and state series converging to the $^2\Pi_{1/2}$ spin–orbit components of the ground state molecular ions. The analyses allowed determination of rotational and vibrational spectroscopic parameters for the excited electronic states. Furthermore (3+1) REMPI spectra of HCl and DCl, involving three-photon transitions to the m($^3\Pi_1$) state, are also recorded and analysed for the first time. Relative rotational line intensities are used to propose a mechanism for the three-photon absorption transitions based on comparison with line strength predictions.

2. Experimental

The experimental set-up was similar to that which has been described before [12–14]. Tunable UV laser pulses were generated by a Lumonics Hyperdye 300 laser pumped by XeCl/308 nm laser pulses from a Lumonics 510 excimer laser. The bandwidth of the laser beam was about $0.05\,cm^{-1}$. The working wavelength range (332–338 nm) was obtained by using the dye LD-690 and frequency doubling with a KDP-D crystal. The laser pulses were deflected by 90° by a Pellin Broca prism and focused midway between two stainless steel elec-

* Author for correspondence. e-mail: agust@hi.is

Molecular Physics ISSN 0026–8976 print/ISSN 1362–3028 online © 2002 Taylor & Francis Ltd
http://www.tandf.co.uk/journals
DOI: 10.1080/0026897021014878 7

trodes (15 mm diameter and about 20 mm apart) inside a simple glass ionization cell. The electrodes were typically kept at ±250 V. Gas sample pressure in the region 1–5 torr was chosen by maximizing the signal due to ionization. Gas samples from lecture bottles (Merck, HCl: 99.5%; Isotec Inc., DCl: 99%) were thoroughly degassed by a series of freeze, pump and thaw cycles and transferred to the ionization cell at room temperature. Voltage drop pulses from the electrodes, following laser ionization, were amplified by a balanced bias differential amplifier [15], integrated by an integration circuit. Typically 100 pulses (20 Hz laser repetition rate; 5 s sampling time) were sampled and averaged by a LeCroy 9310A, 400 MHz storage oscilloscope and fed into a computer for spectra display and manipulation (software: Test Point, Capital Equipment Corporation). The dye laser output was scanned in 0.05–0.2 cm^{-1} steps for recording spectra. Care was taken to prevent power broadening by minimizing laser power. Calibration of the wavelength was achieved by recording REMPI spectra of chlorine and bromine atomic lines [1, 8]. The accuracy of the calibration was found to be about ±2 cm^{-1} on the three-photon wavenumber scale. Spectral intensities were corrected for possible intensity drift during the scan. Furthermore, the effect of varying laser power was corrected for by dividing the measured intensity by the power cubed.

3. Spectral analysis

Identification and assignments of excited electronic states were based on the rotational structure of vibrational bands in terms of *positions* and *intensities* of rotational lines. Rotational and vibrational parameters were derived from simulation analysis of the spectra, based on least-squares analysis of line positions.

Rotational line *positions* ($\tilde{\nu}_{J',v'\ J'',v''}(i)$) for an isotopomer i ($i = 1$ and 2, refer to ^{1}HCl and ^{2}HCl (i.e. DCl) respectively) are derived from the expression

$$\tilde{\nu}_{J',v'\ J'',v''}(i) = \tilde{\nu}^0_{v'\ v''}(i) + \Delta E_{J',J''}(i), \tag{1}$$

where $\tilde{\nu}^0_{v'\ v''}(i)$ is the band origin of a vibrational band. $\Delta E_{J',J''}(i)$ is the difference in rotational energies in the ground and the excited states [1, 7]. The band origin of an isotopomer i can be expressed as [16]

$$\begin{aligned}\tilde{\nu}^0_{v'\ v''}(i) = T'_e &+ \{\omega'_e(i)(v'+\tfrac{1}{2}) - \omega_e x'_e(i)(v'+\tfrac{1}{2})^2\} \\ &- \{\omega''_e(i)(v''+\tfrac{1}{2}) - \omega_e x''_e(i)(v''+\tfrac{1}{2})^2\},\end{aligned} \tag{2}$$

where $\omega'_e(i)$ and $\omega''_e(i)$ are the vibrational frequencies for the excited state and the ground state, respectively and $\omega_e x'_e(i)$ and $\omega_e x''_e(i)$ are the corresponding anharmonicity constants. T'_e is the electronic energy minimum for the excited state potential. Given the standard relationship between the vibrational frequencies and the anharmonicity constants for the different isotopomers, based on the ratio of the reduced masses ($\mu(1)/\mu(2)$) [17],

$$\omega_e(2) = \omega_e(1)\rho, \tag{3}$$

$$\omega_e x_e(2) = \omega_e x_e(1)\rho^2, \tag{4}$$

where

$$\rho = [\mu(1)/\mu(2)]^{1/2}, \tag{5}$$

the spacing between spectral origins/isotope shift ($\Delta\tilde{\nu}^0$) can be expressed as

$$\begin{aligned}\Delta\tilde{\nu}^0 &= [\omega'_e(1)(v'+\tfrac{1}{2}) - \omega''_e(1)(v''+\tfrac{1}{2})][1-\rho] \\ &\quad - [\omega_e x'_e(1)(v'+\tfrac{1}{2})^2 \\ &\quad - \omega_e x''_e(1)(v''+\tfrac{1}{2})^2][1-\rho^2],\end{aligned} \tag{6}$$

$$\sim [\omega'_e(1)(v'+\tfrac{1}{2}) - \omega''_e(1)(v''+\tfrac{1}{2})][1-\rho]. \tag{7}$$

The difference in the rotational energies for isotopomer i ($\Delta E_{J',J''}(i)/cm^{-1}$) is defined as

$$\begin{aligned}\Delta E_{J',J''}(i) &= (J+\Delta J)(J+\Delta J+1)B_{v'}(i) \\ &\quad - (J+\Delta J)^2(J+\Delta J+1)^2 D_{v'}(i) \\ &\quad - J(J+1)B_{v''}(i) + J^2(J+1)^2 D_{v''}(i).\end{aligned} \tag{8}$$

$B_{v'}(i)$, $D_{v'}(i)$, $B_{v''}(i)$ and $D_{v''}(i)$ are the rotational constants for the upper and lower states, respectively. $J = J''$ and $\Delta J(= J' - J'')$ is −3, −2, −1, 0, +1, +2 and +3 for the N, O, P, Q, R, S and T branches, respectively. The standard relationship between the rotational constants is

$$B_v(2) = B_v(1)\rho^2, \tag{9}$$

$$D_v(2) = D_v(1)\rho^4, \tag{10}$$

$$D_v = 4B_v^3/\omega_e^2. \tag{11}$$

Relative line *intensities* (I_{rel}) of spectra recorded at thermal equilibrium are evaluated from

$$I_{rel} = CS_{\Delta\Omega} \exp(-E(J'')hc/k_B T), \tag{12}$$

where $S_{\Delta\Omega}$ is the three-photon absorption strength. $E(J'')$ is the rotational energy in the ground state (in cm^{-1}), h is Planck's constant, c is the speed of light, k_B is the Boltzmann constant, T is the temperature in K and C is an arbitrary constant. The three-photon absorption strength, $S_{\Delta\Omega}$, is expressed as

$$S_{\Delta\Omega} = s_1\mu_1^2 + s_3\mu_3^2, \tag{13}$$

where s_1 and s_3 are Hönl–London type [17] functions of the ground and the excited states' total angular momentum quantum numbers (J'' and J') and of the total electronic angular momentum projection quantum numbers (Ω'' and Ω') [1]. μ_1^2 and μ_3^2 are sum and

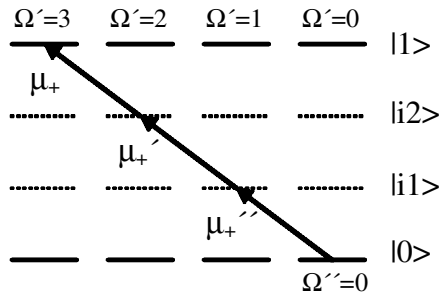

Figure 1. The path for the three-photon absorption transition $\Omega' = 3 \quad \Omega'' = 0$ via virtual states ($\Omega_{i2} = 2$ and $\Omega_{i1} = 1$). Transition dipole moments (μ_+, μ_+', μ_+'') are indicated.

product functions of $\mu_\parallel$ and $\mu_\pm$ values, which represent the collective effect of all one-photon transition moments and energy denominators that give rise to parallel or perpendicular transitions, respectively [2, 18]. The subscript numbers 1 and 3 refer to the order of Clebsch–Gordan coefficients, in terms of which s_1 and s_3 can be written [18–20]. μ_1^2 and μ_3^2 are treated as variables in simulation analyses to determine the relative values μ_1^2/μ_3^2 (see below).

In the case of an $\Omega' = 3 \quad \Omega'' = 0$ three-photon transition the first term on the right-hand side of equation (13) equals zero and the absorption strength is simply expressed as

$$S_{\Delta\Omega} = s_3(\mu_+\mu_+'\mu_+'')^2. \tag{14}$$

The product function inside the bracket represents the one and only excitation channel via the virtual states $|i1\rangle$ ($\Omega = 1$) and $|i2\rangle$ ($\Omega = 2$) as demonstrated in figure 1. The s_3 functions [1] are plotted against J ($= J''$) for the different rotational line series ($N(\Delta J = -3)$ to $T(\Delta J = 3)$) shown in figure 2. These plots show the relative intensities of the rotational line series for low J ($J < 15$). Thus the R and the Q branch lines are found to be of largest intensity. Characteristically, rotational line intensities vary in parallel fashion for line series with the same $|\Delta J|$ value but opposite signs (N and T; O and S; P and R). However, the line intensities vary as $-|\Delta J| < |\Delta J|$ (i.e. N<T; O<S; P<R). Furthermore, the lowest J for non-zero s_3 values ($J_{\min}$) varies with ΔJ (line series) as [1]

$$J_{\min} = 3 - \Delta J. \tag{15}$$

4. Results and analysis

The frequency range where single-colour (3 + 1) REMPI spectra of HCl and DCl are expected to be observed is determined by the molecular ionization energies (IP: 12.748 eV/$\overline{\text{IP}}$: 102 820 cm^{-1} [21]). The minimum and maximum laser wavenumbers ($\tilde{\nu}_{\text{LASER}}$) for (3 + 1) REMPI correspond to the photon energies which equal one fourth and one third of the ionization potential, respectively. Therefore the excitation wavenumber range ($\tilde{\nu}_{\text{exc}} = 3\tilde{\nu}_{\text{LASER}}$) for (3 + 1) REMPI of HCl and DCl is

$$77\,115 < \tilde{\nu}_{\text{exc}}/\text{cm}^{-1} < 102\,820.$$

Figure 3 (*a*) shows the REMPI spectrum of HCl in the excitation wavenumber range 89 750–90 350 cm^{-1}. Two overlapping vibrational bands centred at 89 981.6 cm^{-1} and 90 133.8 cm^{-1} are found in this region. The one observed at 90 133.8 cm^{-1} was identified as the (3 + 1) REMPI spectrum of the (0, 0) vibrational band of the $m^3\Pi_1 \quad X(^1\Sigma^+)$ electronic transition by comparison with previous observations in single-photon absorption [22, 23] and in (2 + 1)REMPI [24, 25] and from spectral simulations (see figures 3 and 4). The separated experimental spectra (figures 3 (*b*) and (*c*) and figures 4 (top) and 5 (top)) were formed by plotting peaks which belong

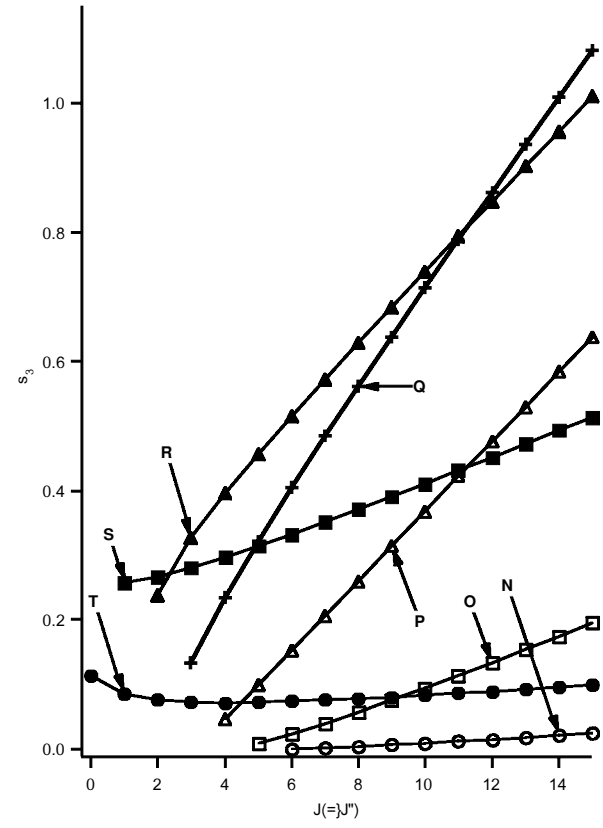

Figure 2. Relative three-photon rotational line strengths (s_3) for rotational branches (N...T) as functions of the total angular momentum quantum numbers (J) for the three-photon electronic transition $\Omega' = 3 \quad \Omega'' = 0$.

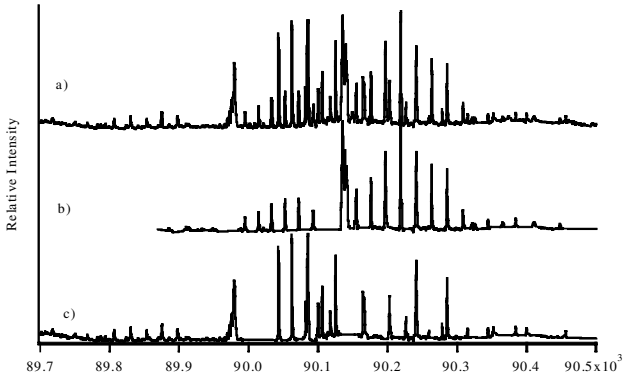

Figure 3. Experimental (3+1) REMPI spectrum of HCl (top) due to the three-photon transitions $m(^3\Pi_1) \quad X(^1\Sigma^+)$, (0,0) (middle) and $L(^1\Phi_3) \quad X(^1\Sigma^+)$, (0,0) (bottom). Separation of spectral bands (b and c) is based on the analysis mentioned in the text and shown in figures 4 and 5.

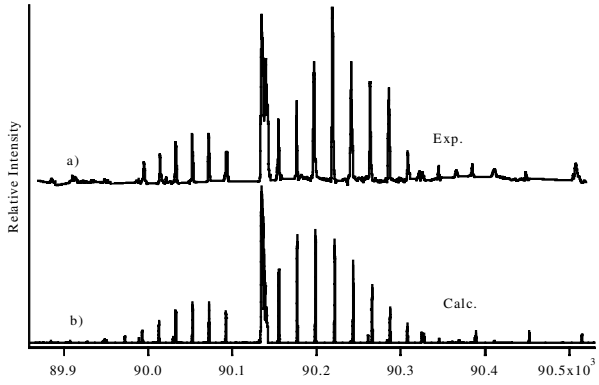

Figure 4. HCl, $m(^3\Pi_1) \quad X(^1\Sigma^+)$, (0,0) (3+1) REMPI spectrum simulation: (*a*) experimental spectrum and (*b*) calculated spectrum.

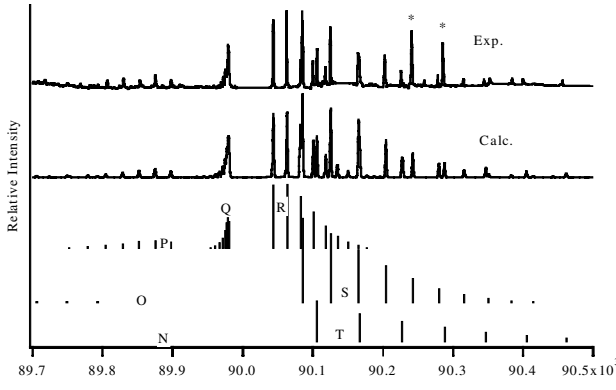

Figure 5. HCl, $L(^1\Phi_3) \quad X(^1\Sigma^+)$, (0,0) (3+1) REMPI spectrum simulation. Experimental spectrum (top), calculated rotational line contributions (bottom) and simulated spectrum (underneath the experimental spectrum). Line overlap is observed for peaks marked with asterisks.

to one of the two bands only, eliminating those belonging to the other band. Spectral regions where peaks have been eliminated have been replaced by straight lines. The spectrum centred at 89 981.6 cm^{-1} shows the intensity patterns for rotational line series to be expected for an $\Omega' = 3 \quad \Omega'' = 0$ transition (see above). Simulation analyses, shown in figure 5, revealed the spectroscopic parameters, $\tilde{\nu}^0$, B' and D' listed in table 1 along with values obtained by others. Furthermore, for the 90 133.8 cm^{-1} system, the best fit was obtained for $\mu_1^2/\mu_3^2 = 1.1 \pm 0.1$. The $\Omega = 3$ state ($\tilde{\nu}^0 = 89\,981.6\,\text{cm}^{-1}$) has not been observed before. We assign it to the $L(^1\Phi_3)$ state ($v' = 0$) which belongs to the dδ manifold ($(\sigma^2\pi^3)3\text{d}\delta$) and Rydberg series converging to the higher energy $^2\Pi_{1/2}$ spin–orbit component of the ground ionic state ($X(^2\Pi_\Omega)$), for the following reasons. First, this state is close to the $K(^1\Pi_1)$ state ($\tilde{\nu}^0 = 89\,680.5\,\text{cm}^{-1}$ [23, 24]) which belongs to this same manifold and converges to the same spin–orbit component. Secondly, another $\Omega = 3$ state has been observed lower in energy by about 800 cm^{-1} [26]. The spacing between these two $\Omega = 3$ states is of the same order of magnitude as that of the spin–orbit splitting, 648 cm^{-1} [21], for the ground state ion, suggesting that the latter belongs to the same manifold ($(\sigma^2\pi^3)3\text{d}\delta$) but converges to the lower energy spin–orbit component of the ground ionic state ($^2\Pi_{3/2}$) [1, 2]. Thirdly, the similarity in rotational parameters observed for this state and the ground state ($B' = 10.40\,\text{cm}^{-1}$ and $B'' \approx 10.44\,\text{cm}^{-1}$), implying comparable average internuclear distances for the two potential curves, suggests that the (0,0) band will be the dominant vibrational band.

Despite the manufacturer's guaranteed purity of 99% for the DCl gas sample used, a close to 1:1 ratio of DCl and HCl gases was observed in our (3+1) REMPI spectra. Spectra due to the $L(^1\Phi_3) \quad X(^1\Sigma^+)$ and $m(^3\Pi_1) \quad X(^1\Sigma^+)$ transitions for both compounds were observed in the region 89 750 to 90 350 cm^{-1}. These were separated, in a similar fashion to that shown for HCl in figure 3, for further simulation analysis. Resulting spectroscopic parameters, $\tilde{\nu}^0$, B' and D', are listed in table 1. Furthermore, vibrational frequencies (in wavenumbers) of the excited states for both compounds ($\omega_e'(1)$ and $\omega_e'(2)$) could be estimated from the isotope shift ($\Delta\tilde{\nu}^0$) by rearranging equation (7)

$$\omega_e'(1) = \frac{2\Delta\tilde{\nu}^0}{(1-\rho)} + \omega_e''(1) \tag{16}$$

and substituting into equation (3). The resulting values are listed in table 1.

Five major excitation channels are involved in $\Omega' = 1 \quad \Omega'' = 0$ transitions:

Table 1. Band origins ($\tilde{\nu}^0$) vibrational frequencies (ω_e) and rotational parameters (B and D) for HCl and DCl states.

				ν^0		ω_e		B (cm^{-1})		D $\times 10^3$ (cm^{-1})	
Comp.	State	Configs.	Ion core	Ours	Others	Ours	Others	Ours	Others	Ours	Others
HCl	$X(^1\Sigma^+)$	$\sigma^2\pi^4$	—	—	—	—	2990.9463[a]	—	10.439 826[a]		0.508 771 23[a]
HCl	$L(^1\Phi_3)$	$\sigma^2\pi^3 3d\delta$	$^2\Pi_{1/2}$	89 981.6	—	2471.8		10.3	—	1.15	—
HCl	$m(^3\Pi_1)$	$\sigma^2\pi^3 e\sigma$	$^2\Pi_{3/2}$	90 133.83(e,f)	90 133.53(8)(e)[b]	2747.9		10.61(e)	10.626 3(9)(e)[b]	1.00(e)	1.191 11(29)(e)[b]
					90 133.63(13)(f)[b]			10.65(f)	10.690 2(17)(f)[b]	2.10(f)	2.677 1(9)(f)[b]
					90 133.4(e)[c]				10.62(e)[c]		1.00(e)[c]
									10.68(f)[c]		2.41(f)[c]
DCl	$X(^1\Sigma^+)$	$\sigma^2\pi^4$	—				2145.163[a]	—	5.392 15[a]		0.136 277 77[a]
DCl	$L(^1\Phi_3)$	$\sigma^2\pi^3 3d\delta$	$^2\Pi_{1/2}$	90 055	—	1772.8		5.22		0.354 30	
DCl	$m(^3\Pi_1)$	$\sigma^2\pi^3 e\sigma$	$^2\Pi_{3/2}$	90 168.2(e,f)	—	1970.8		5.296(e)		0.285(e)	
								5.278(f)		0.38(f)	

[a] See [21].
[b] See [24].
[c] See (22).

Table 2. Transition moment functions (μ_1^2 and μ_3^2) and ratios (μ_1^2/μ_3^2) for the five major channels (see text) in $\Omega' = 1 \quad \Omega'' = 0$ three-photon absorption.

Channel	$\Omega(\lvert 1\rangle)$	$\Omega(\lvert i2\rangle)$	$\Omega(\lvert i1\rangle)$	$\Omega(\lvert 0\rangle)$	μ_1^2	μ_3^2	μ_1^2/μ_3^2
1	1	0	0	0	$(9/25)\{\mu_+\mu'_\parallel\mu''_\parallel\}^2$	$4\{\mu_+\mu'_\parallel\mu''_\parallel\}^2$	0.09
2	1	1	0	0	$(9/25)\{\mu_\parallel\mu'_+\mu''_\parallel\}^2$	$4\{\mu_\parallel\mu'_+\mu''_+\}^2$	0.09
3	1	1	1	0	$(9/25)\{\mu_\parallel\mu'_\parallel\mu''_+\}^2$	$4\{\mu_\parallel\mu'_\parallel\mu''_+\}^2$	0.09
4	1	0	1	0	$(36/25)\{\mu_+\mu'_-\mu''_+\}^2$	$1\{\mu_+\mu'_-\mu''_+\}^2$	1.44
5	1	2	1	0	$(36/25)\{\mu_-\mu'_+\mu''_+\}^2$	$1\{\mu_-\mu'_+\mu''_+\}^2$	1.44

(1) $\{\Omega'_1 = 1\} \overset{\mu_+}{-} \{\Omega'_{i2} = 0\} \overset{\mu'_\parallel}{-} \{\Omega'_{i1} = 0\} \overset{\mu''_\parallel}{-} \{\Omega''_0 = 0\}$,

(2) $\{\Omega'_1 = 1\} \overset{\mu_\parallel}{-} \{\Omega'_{i2} = 1\} \overset{\mu'_+}{-} \{\Omega'_{i1} = 0\} \overset{\mu''_\parallel}{-} \{\Omega''_0 = 0\}$,

(3) $\{\Omega'_1 = 1\} \overset{\mu_\parallel}{-} \{\Omega'_{i2} = 1\} \overset{\mu'_\parallel}{-} \{\Omega'_{i1} = 1\} \overset{\mu''_+}{-} \{\Omega''_0 = 0\}$,

(4) $\{\Omega'_1 = 1\} \overset{\mu_+}{-} \{\Omega'_{i2} = 0\} \overset{\mu'_-}{-} \{\Omega'_{i1} = 1\} \overset{\mu''_+}{-} \{\Omega''_0 = 0\}$,

(5) $\{\Omega'_1 = 1\} \overset{\mu_-}{-} \{\Omega'_{i2} = 2\} \overset{\mu'_+}{-} \{\Omega_{i1} = 1\} \overset{\mu''_+}{-} \{\Omega''_0 = 0\}$,

where the subscript numbers 1 and 0 refer to the resonance excited state and the ground state, respectively and $i2$ and $i1$ refer to virtual intermediate states. Relevant expressions for μ_1^2 and μ_3^2 as well as values for μ_1^2/μ_3^2 ratios derived from [2] are to be found in table 2. The observed ratio for the m($^3\Pi_1$) X($^1\Sigma^+$) transition ($\mu_1^2/\mu_3^2 = 1.1 \pm 0.1$) differs from those predicted for the major channels (0.09 for 1–3 and 1.44 for 4 and 5) suggesting that the excitation mechanism involves combination of more than one channel, the opposite of what has been suggested for the $\Omega' = 0 \quad \Omega'' = 0$ transition E($^1\Sigma^+$) X($^1\Sigma^+$) ($\tilde{\nu}^0 = 83\,781\ \mathrm{cm}^{-1}$) in HCl [2].

5. Conclusions

Simulation calculations based on Hönl–London-type expressions for rotational line strengths in three-photon absorptions allowed identification and characterization of the first observed $\Omega = 3$ states in HCl and DCl in (3+1) REMPI spectra. The states are assigned as the L($^1\Phi_3$) Rydberg states for vibrational quantum numbers $v' = 0$ and electronic configurations $(\sigma^2\pi^3)3d\delta$ which belong to series converging to the $\Omega = 1/2$ spin–orbit component of the ground state molecular ions (X($^2\Pi_\Omega$)). The analyses allowed evaluation of band origins and rotational constants for the excited states. Simulation analysis of the (3+1) REMPI spectra due to the three-photon transitions m($^3\Pi_1$) X($^1\Sigma^+$) in HCl and DCl resulted in spectroscopic parameters some of which, for HCl, could be compared with previous data. Reasonably good agreement was found between our data and those determined by others in single- or two-photon absorption experiments. The difference in band origins for the two isotopomers (HCl and DCl), i.e. the isotope shift, was used to evaluate vibrational frequencies of the excited states for both molecules. Transition moment function parameters were evaluated from the (3+1) REMPI spectra due to the m X transition in HCl. These were interpreted in terms of the effect of intermediate states on the three-photon excitation mechanism.

The financial support of the University Research Fund, University of Iceland and the Icelandic Science Foundation is gratefully acknowledged. We would also like to thank Benedikt G. Waage and Jón Matthíasson for useful help with this project.

References

[1] Kvaran, Á., Waage, B. G., and Wang, H., 2000, *J. chem. Phys.*, **113,** 1755.
[2] Kvaran, Á., Wang, H., and Waage, B. G., 2001, *Can. J. Phys.*, **79,** 197.
[3] Ascenzi, D., Langford, S., Ashfold, M., and Orr-Ewing, A., 2001, *Phys. Chem. chem. Phys.*, **3,** 29.
[4] Green, D. S., Bickel, G. A., and Wallace, S. C., 1991, *J. molec. Spectrosc.*, **150,** 354.
[5] Green, D. S., and Wallace, S. C., 1992, *J. chem. Phys.*, **96,** 5857.
[6] Xie, Y., Reilly, P. T. A., Chilukuri, S., and Gordon, R. J., 1991, *J. chem. Phys.*, **95,** 854.
[7] Kvaran, Á., Logadóttir, Á., and Wang, H., 1998, *J. chem. Phys.*, **109,** 5856.
[8] Kvaran, Á., Wang, H., and Logadóttir, Á., 2000, *J. chem. Phys.*, **112,** 10811.
[9] Callaghan, R., and Gordon, R. J., 1990, *J. chem. Phys.*, **93,** 4624.
[10] Wang, H., and Kvaran, Á., 2001, *J. molec. Struct.*, **563–564,** 235.
[11] Donovan, R. J., Flexen, A. C., Lawley, K. P., and Ridley, T., 1998, *Chem. Phys.*, **226,** 217.
[12] Kvaran, Á., Wang, H., and Logadóttir, Á., 1998, *Recent Research Developments in Physical Chemistry*, Vol. 2 (Indian Academy of Sciences, Bangalore: Transworld Research Network), pp. 233–244.
[13] Huasheng, W., Asgeirsson, J., Kvaran, Á., Donovan, R. J., Flood, R. V., Lawley, K. P., Ridley, T., and Yencha, A. J., 1993, *J. molec. Struct.*, **293,** 217.
[14] Kvaran, Á., Wang, H., and Zsgeirsson, J., 1994, *J. molec. Spectrosc.*, **163,** 541.

[15] Adams, T. E., Morrison, R. J. S., and Grant, E. R., 1980, *Rev. sci. Instrum.*, **51,** 141.
[16] Kvaran, Á., Wang, H., and Jóhannesson, G. H. J., 1995, *J. phys. Chem.*, **99,** 4451.
[17] Herzberg, G., 1950, *Molecular Spectra and Molecular Structure; I. Spectra of Diatomic Molecules, 2nd Edn (New York: Van Nostrand Reinhold Company)*.
[18] Halpern, J. B., Aacharias, H., and Wallenstein, R., 1980, *J. molec. Spectrosc.*, **79,** 1.
[19] Condon, E. U., and Shortley, G. H., 1963, *The Theory of Atomic Spectra (Cambridge: Cambridge University Press)*.
[20] Falkoff, D. L., Colladay, G. S., and Sells, R. E., 1952, *Can. J. Phys.*, **30,** 253.
[21] Huber, K. P., and Herzberg, G., 1979, *Constants of Diatomic Molecules* (New York: Van Nostrand-Reinhold).
[22] Douglas, A. E., and Greening, F. R., 1979, *Can. J. Phys.*, **57,** 1650.
[23] Ginter, D. S., and Ginter, M. L., 1981, *J. molec. Spectrosc.*, **90,** 177.
[24] Green, D. S., Bickel, G. A., and Wallace, S. C., 1991, *J. molec. Spectrosc.*, **150,** 303.
[25] Green, D. S., Bickel, G. A., and Wallace, S. C., 1991, *J. molec. Spectrosc.*, **150,** 388.
[26] Kvaran, Á., and Wang, H., in preparation, to be published.